Journal of Thermal Analysis and Calorimetry, Vol. 88 (2007) 1, 193–200

OBTAINING OF $Ni_{0.65}Zn_{0.35}Fe_2O_4/SiO_2$ NANOCOMPOSITES BY THERMAL DECOMPOSITION OF COMPLEX COMPOUNDS EMBEDDED IN SILICA MATRIX

Marcela Stoia[1*], *C. Caizer*[2], *M. Stefanescu*[1], *P. Barvinschi*[2] *and I. Julean*[1]

[1]Faculty of Industrial Chemistry and Environmental Engineering, University 'Politehnica' of Timişoara, P-ta Victoriei nr. 2. 300006 Timişoara, Romania
[2]Faculty of Physics, West University of Timişoara, Bv. V. Parvan no. 4, 300223 Timişoara, Romania

This article presents the results of our investigation on the obtaining of $Ni_{0.65}Zn_{0.35}Fe_2O_4$ ferrite nanoparticles embedded in a SiO_2 matrix using a modified sol–gel synthesis method, starting from tetraethylorthosilicate (TEOS), metal (Fe^{III},Ni^{II},Zn^{II}) nitrates and ethylene glycol (EG). This method consists in the formation of carboxylate type complexes, inside the silica matrix, used as forerunners for the ferrite/silica nanocomposites. We prepared gels with different compositions, in order to obtain, through a suitable thermal treatment, the nanocomposites $(Ni_{0.65}Zn_{0.35}Fe_2O_4)_x$–$(SiO_2)_{100-x}$ (where x=10, 20, 30, 40, 50, 60 mass%). The synthesized gels were studied by differential thermal analysis (DTA), thermogravimetry (TG) and FTIR spectroscopy.

The formation of Ni–Zn ferrite in the silica matrix and the behavior in an external magnetic field were studied by X-ray diffraction (XRD) and quasi-static magnetic measurements (50 Hz).

Keywords: *ethylene glycol, magnetic, Ni,Zn ferrite, sol–gel*

Introduction

Nanomaterials constitute, nowadays, an intensively studied class of materials, due to their remarkable properties, compared to the properties of the bulk material obtained by conventional methods [1–3].

The amorphous matrixes play an important role to lower the motion of the particles and the granules growth during the nanocrystals formation [4]. The nanocrystals dispersed in this kind of matrixes present a limited agglomeration and a narrow size distribution, under the effect of spatial contraction. Moreover, the morphology, the particle size distribution and the nanocrystals structure may be controlled by the modification of the matrixes composition, of the dispersed phase concentration and by the thermal treatment conditions [5–7].

Therefore, this nanocomposites present a special interest due to their particular properties (optical, catalytic, magnetic, etc.) [8, 9]. This is the reason why the sol–gel method is widely used and why it has different practical alternatives.

The nanocomposites obtained by embedding the Ni–Zn ferrite nanoparticles in inorganic matrixes, are of great interest due to their performant chemical, electrical and magnetic properties, as a result of their particulate structure [5–7, 10, 11].

Different variants of the sol-gel processing have been developed in order to obtain finer Ni,Zn ferrite nanoparticles, dispersed in a SiO_2 matrix, at low temperatures.

In this paper we present a study regarding the obtaining of $(Ni_{0.65}Zn_{0.35}Fe_2O_4)_x/(SiO_2)_{100-x}$ nanocomposites (where x=10, 20, 30, 40, 50, 60 mass%), by thermal decomposition of glyoxylate precursors in the silica matrix. The magnetic properties of the obtained nanocomposites depend on the ferrites concentration in the matrix, which determines the dispersion degree and the dimensions of the ferrite nanoparticles.

Experimental

Materials

For the liquid phase synthesis, we used tetraethylorthosilicate (TEOS) (Merck, 98%), metallic nitrates (MN) (Fluka (p.a.)): $Fe(NO_3)_3 \cdot 9H_2O$, $Zn(NO_3)_2 \cdot 6H_2O$, $Ni(NO_3)_2 \cdot 6H_2O$, ethylene glycol (EG) (Fluka) and ethanol (EtOH) (98%).

We have synthesized three types of gels, all in acid catalysis (HNO_3):

- TEOS–EG–MN (samples E_1, E_2, E_3, E_4, E_5 E_6)
- TEOS–EG–H_2O (samples G_1, G_2, G_3, G_4, G_5, G_6)
- TEOS–EG–MN–H_2O (samples M_1, M_2, M_3, M_4, M_5, M_6)

* Author for correspondence: marcela.stoia@chim.upt.ro

1388–6150/$20.00

Akadémiai Kiadó, Budapest, Hungary
Springer, Dordrecht, The Netherlands

Synthesis of TEOS–EG–MN gels

The ethanolic TEOS solution was dropped, under intense stirring, to the ethanol–metal nitrates-ethylene glycol solution (for a molar ratio EG:NO_3^-=1:1). During the stirring, EtOH was also added, until the two solutions were completely homogenized. After a 30 min stirring the obtained clear solution (sol) was left to gel at room temperature. The characteristics of the gels, obtained after the gelling process (E_1, E_2, E_3, E_4, E_5, E_6), are presented in Table 1. The gels were dried at 40°C, for 6 h, and then thermally treated at 130°C, for 6 h, when the redox reaction takes place, forming the complex combination.

The existing water, in these gels, is only the crystallization water of the metal nitrates.

Synthesis of TEOS–EG–H_2O gels

In order to study the effect of EGs presence in the system TEOS–H_2O, the gels G_1, G_2 G_3, G_4, G_5, G_6, of different compositions, were prepared. These correspond to the gels E_i, but without metal nitrates (Table 1). The amount of added water is identical to the one pro-

Table 1 Compositions and characteristics of the synthesized gels

Sample	Quantity/mol							
						H_2O		
	$Ni(NO_3)_2{\cdot}6H_2O$	$Zn(NO_3)_2{\cdot}6H_2O$	$Fe(NO_3)_3{\cdot}9H_2O$	NO_3^-	TEOS	n_1 (introduced in synthesis)	n_2 (from metal nitrates)	n_{total}
E_1	$1.37{\cdot}10^{-3}$	$7.39{\cdot}10^{-4}$	$4.22{\cdot}10^{-3}$	0.0169	0.0750	–	0.0507	0.0507
E_2	$2.74{\cdot}10^{-3}$	$1.48{\cdot}10^{-3}$	$8.44{\cdot}10^{-3}$	0.0338	0.0667	–	0.101	0.101
E_3	$4.12{\cdot}10^{-3}$	$2.22{\cdot}10^{-3}$	0.0127	0.0507	0.0583	–	0.152	0.152
E_4	$5.491{\cdot}10^{-3}$	$2.96{\cdot}10^{-3}$	0.0169	0.0675	0.0500	–	0.203	0.203
E_5	$6.86{\cdot}10^{-3}$	$3.69{\cdot}10^{-3}$	0.0211	0.0844	0.0417	–	0.253	0.253
E_6	$8.23{\cdot}10^{-3}$	$4.43{\cdot}10^{-3}$	0.0253	0.101	0.0333	–	0.304	0.304
G_1	–	–	–	–	0.0750	0.0507	–	0.0507
G_2	–	–	–	–	0.0667	0.101	–	0.101
G_3	–	–	–	–	0.0583	0.152	–	0.152
G_4	–	–	–	–	0.0500	0.203	–	0.203
G_5	–	–	–	–	0.0417	0.253	–	0.253
G_6	–	–	–	–	0.0333	0.304	–	0.304
M_1	$1.37{\cdot}10^{-3}$	$7.39{\cdot}10^{-4}$	$4.22{\cdot}10^{-3}$	0.0169	0.0750	0.300	0.0507	0.350
M_2	$2.74{\cdot}10^{-3}$	$1.48{\cdot}10^{-3}$	$8.44{\cdot}10^{-3}$	0.0338	0.0667	0.267	0.101	0.368
M_3	$4.12{\cdot}10^{-3}$	$2.22{\cdot}10^{-3}$	0.0127	0.0507	0.0583	0.233	0.152	0.385
M_4	$5.491{\cdot}10^{-3}$	$2.96{\cdot}10^{-3}$	0.0169	0.0675	0.0500	0.200	0.203	0.403
M_5	$6.86{\cdot}10^{-3}$	$3.69{\cdot}10^{-3}$	0.0211	0.0844	0.0417	0.167	0.253	0.420
M_6	$8.23{\cdot}10^{-3}$	$4.43{\cdot}10^{-3}$	0.0253	0.101	0.0333	0.133	0.304	0.437

Sample	Quantity/mol				Molar ratio	t_g/h
	EG			EtOH	TEOS:H_2O:NO_3:EG	
	$n_1=n(NO_3^-)$	$n_2=n$(TEOS)	$n_{total}=n_1+n_2$			
E_1	0.0169	–	0.0169	0.130	1:0.68:0.24:0.24	136
E_2	0.0338	–	0.0338	0.130	1:1.51:0.50:0:50	46
E_3	0.0507	–	0.0507	0.150	1:2.61:0.87:0.87	158
E_4	0.0675	–	0.0675	0.170	1:4.06:1.35:1.35	177
E_5	0.0844	–	0.0844	0.190	1:6.07:2.02:2.02	204
E_6	0.101	–	0.101	0.200	1:9.13:3.03:3.03	198
G_1	0.0169	–	0.0169	0.130	1:0.68:0.00:0.24	96
G_2	0.0338	–	0.0338	0.130	1:1.51:0.00:0.50	54
G_3	0.0507	–	0.0507	0.150	1:2.61:0.00:0.87	123
G_4	0.0675	–	0.0675	0.170	1:4.06:0.00:1.35	148
G_5	0.0844	–	0.0844	0.190	1:6.07:0.00:2.02	174
G_6	0.101	–	0.101	0.200	1:9.13:0.00:3.03	222
M_1	0.0169	0.0750	0.0919	0.150	1:4.66:0.22:1.22	110
M_2	0.0338	0.0667	0.100	0.150	1:5.52:0.51:1.38	134
M_3	0.0507	0.0583	0.109	0.200	1:6.60:0.87:1.87	170
M_4	0.0675	0.0500	0.118	0.220	1:8.06:1.35:2.36	268
M_5	0.0844	0.0417	0.126	0.250	1:10.07:2.02:3.02	216
M_6	0.101	0.0333	0.134	0.270	1:13.12:3.03:4.02	258

ceeded from the metal nitrates, in the corresponding E_i gels. These gels were dried at 40°C and then thermally treated at 130°C, for 6 h.

Synthesis of TEOS–EG–MN–H_2O gels

In the second synthesis variant, gels with variable compositions (similar to the gels E_i) were prepared, using supplementary amounts of water and EG, comparing to the first method. The compositions of the gels are also presented in Table 1.

To the solution obtained by dissolving of metal nitrates ($Fe(NO_3)_3 \cdot 9H_2O$, $Zn(NO_3)_2 \cdot 6H_2O$, $Ni(NO_3)_2 \cdot 6H_2O$), in the corresponding water, ethylene glycol and ethanol volume, an ethanolic TEOS solution was dropped, under stirring. During the mixing, another EtOH amount was added in order to obtain a clear solution. After a 30 min stirring, the obtained clear solution (sol) was left to gel at room temperature. After gelling, the obtained gels (M_1, M_2, M_3, M_4, M_5, M_6) were dried at 40°C, for 6 h, when the redox reaction takes place, forming the complex combination.

All the synthesized gels were studied by differential thermal analysis (DTA), thermogravimetric analysis (TG) and FTIR spectrometry.

In order to obtain $(Ni_{0.65}Zn_{0.35}Fe_2O_4)_x/(SiO_2)_{100-x}$ nanocomposites (where x=10, 20, 30, 40, 50, 60 mass%), the samples E_i and M_i, where thermally treated at different temperatures (600–1000°C). The formation of the Ni,Zn ferrite in the silica matrix, its morphology and its behaviour in external magnetic field, were studied by X-ray diffraction (XRD), transmission electron microscopy (TEM) and quasi-static magnetic measurements (50 Hz).

Methods

Thermal analysis of the gels was registered on a 1500 MOM Hungary derivatograph, in the temperature range 20–500°C, with a heating rate of 5°C min^{-1}, having as inert material α-Al_2O_3 and using Pt crucibles in form of plates, in air atmosphere and nitrogen atmosphere, respectively.

The FTIR spectra of the samples, in a powdered form, were carried out with a JASCO 430 FT-IR spectrometer on KBr pellets.

The crystalline phases obtained on the composites were identified by X-ray diffraction in a Bruker advanced diffractometer using CuK_α (λ_{Cu}=1.54056 Å) radiation.

The magnetic behaviour of the Ni–Zn ferrite nanoparticles, dispersed in the silica matrix, was studied at room temperature and magnetic field frequency of 50 Hz. Magnetic measurements were taken with a standard equipment described in [12] provided with a data acquisition system (DAQ) connected to a personal computer (PC).

Results and discussion

In our previous studies, we prepared the Ni, Zn ferrite by thermal decomposition of heteropolynuclear complex combination of glyoxylate type, obtained from the reaction between EG and Fe, Ni, Zn metallic nitrates [13]:

$$2Fe(NO_3)_3+0.65Ni(NO_3)_2+0.35Zn(NO_3)_2+ +2C_2H_4(OH)_2+nH_2O\rightarrow Fe_2Ni_{0.65}Zn_{0.35}(OH)_4(C_2H_2O_4)_2 \cdot nH_2O+ +4NO+4HNO_3 \quad (1)$$

$$Fe_2Ni_{0.65}Zn_{0.35}(OH)_4(C_2H_2O_4)_2 \cdot nH_2O\rightarrow Ni_{0.65}Zn_{0.35}Fe_2O_4+4CO+(4+n)H_2O \quad (2)$$

By this method we obtained ferrite nanoparticles (30 nm) at low temperatures (400°C) [13, 14].

In order to obtain finer ferrite nanoparticles (<10 nm), with controlled shape, size and magnetic properties, we have synthesized nanocomposites $Ni_{0.65}Zn_{0.35}Fe_2O_4/SiO_2$, using a modified sol–gel method. This consists in the synthesis of complex combination of glyoxylate type inner the silica matrix (by the redox reaction EG-NO_3^- which takes place in the pores of the matrix) followed by its thermal decomposition, forming Ni,Zn ferrite in matrix at 600°C [15].

We have studied the influence of ferrites concentration in the silica matrix on the ferrite nanoparticles size, on their dispersion, crystallization degree and on the magnetic properties, in order to obtain Ni,Zn ferrite with special magnetic properties. For this purpose, the synthesized gels (as in Table 1) were studied by thermal analysis and FTIR spectroscopy.

Thermal analysis

Figure 1 presents the TG and DTA curves obtained after heating in air of the gel E_5 dried at 40°C, when the silica matrixes pores contain the mixture of EG and metal nitrates.

During the heating of the gel, in air atmosphere, on the DTA curve is registered an exothermic effect at 110°C, which is attributed to the redox reaction between EG and metal nitrates. As a result of this reaction a complex combination of glyoxylate type forms in the pores of the matrix. This process generates on the TG curve, a mass loss corresponding to the elimination of the reaction products: NO, H_2O. In the range 200–300°C, on the DTA curve, is registered a strong exothermic effect, associated to a mass loss on the TG curve, as a result of the complex combination decomposition.

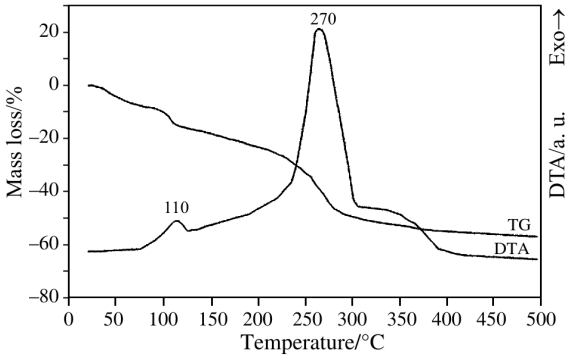

Fig. 1 Thermal curves TG and DTA for E_5 gel, dried at 40°C

Similar processes were observed on the TG and DTA curves for all the synthesized gels: the redox reaction polyol-NO_3^- and the decomposition of the formed complex.

This thermal behavior of the gels (TEOS–EG–MN) resembles to the one obtained by us at thermal analysis of the solutions (EG–MN) [13].

Based on the thermal curves obtained for the gels E_i dried at 40°C, the temperature of 130°C was established as optimal for the synthesis of the complex combination embedded in the silica matrix.

Figure 2 presents the TG and DTA curves registered at heating in air of the gel E_5 (TEOS–EG–MN) thermally treated at 130°C, for 6 h, when the precursor of Ni,Zn ferrite is formed in the pores. Until 200°C, the mass loss corresponds to the elimination of the volatile products from the pores, to the polycondensation reaction of the matrix and to the loss of crystallization water from the complex. The mass loss from the range 200–300°C associated to a strong exothermic effect is due to the oxidative decomposition of the complex, with formation of the metal oxide mixture in the matrix. In this temperature range, processes with mass losses characteristic to the thermal evolution of the silica matrix take also place. The slow mass loss registered until 500°C is due to the promotion of the silica matrix polycondensation process.

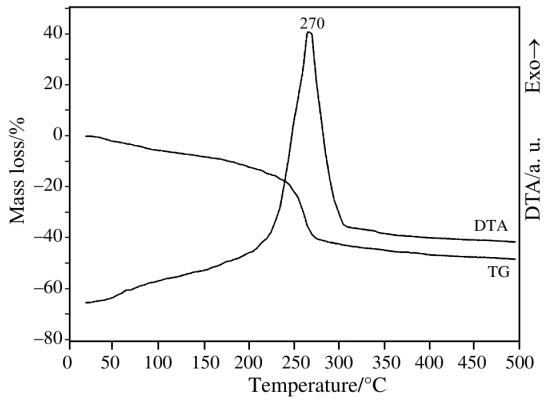

Fig. 2 Thermal curves TG and DTA for E_5 gel, thermally treated at 130°C

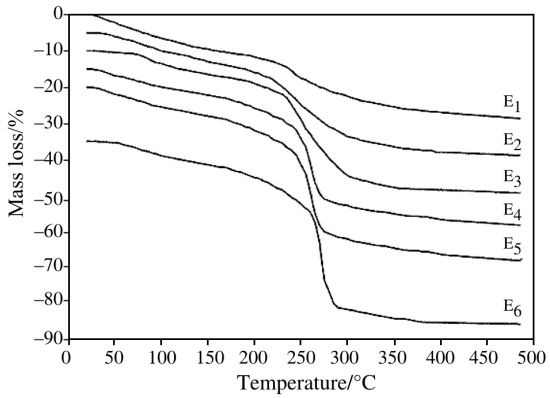

Fig. 3 TG curves of the gels E_i (TEOS–MN–EG) of different compositions thermally treated at 130°C

Figure 3 presents the TG curves registered at air heating, until 500°C, of the gels (TEOS–EG–MN) of different compositions: E_1, E_2, E_3, E_4, E_5, E_6 (Table 1) thermally treated at 130°C, for 6 h. Similar thermal processes are registered for all the gels, the mass losses being dependent, mainly, on the complexes concentration in the matrix.

From our studies on the formation of silica matrix starting from TEOS–EG–H_2O, we have established that EG chemically interacts with the functional groups of the matrix. This leads to the formation of a hybrid matrix which contains organic chains of ≡Si–O–CH_2–CH_2–O–Si≡ type. These organic chains suffer an exothermic oxidative decomposition through thermal treatment in the range 250–300°C [16].

Based on these findings, we consider that the EG used in the synthesis of the E_i gels (TEOS–EG–MN), participates, both at the redox reaction of the complexes formation and in the reaction with the functional groups of silica matrix.

To clear up this aspect, gels G_i (TEOS–EG–H_2O) in molar ratios corresponding to those of the gels E_i were synthesized. These gels were examined by thermal analysis, in air, until 500°C, to follow EG bounding in the matrix.

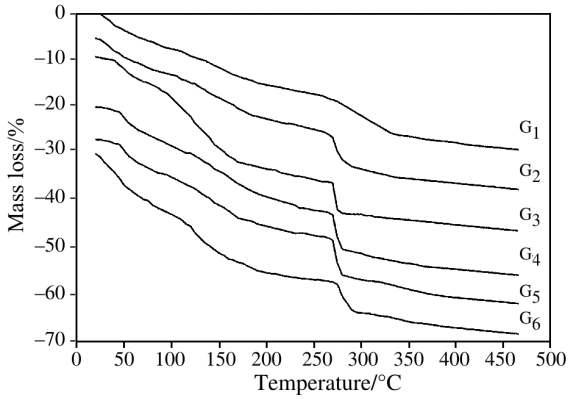

Fig. 4 TG curves of the gels G_i (TEOS–EG–H_2O) of different compositions thermally treated at 130°C

Figure 4 presents the TG curves of the gels G_1, G_2, G_3, G_4, G_5, G_6, thermally treated at 130°C, for 6 h. One can see that all the studied gels present a mass loss in the range 250–300°C, corresponding to the decomposition of the organic chains resulted after the chemical bounding of EG in the matrix. These losses depend on the amount of EG introduced in synthesis.

One may conclude that a part of EG introduced in the synthesis of the gels E_i (TEOS–EG–MN), may be consumed during the formation of the matrix, affecting the quantitative formation of the glyoxylate compounds.

In order to avoid this drawback, we have synthesized gels (TEOS–EG–MN–H_2O) of different compositions (samples M_i), adding a supplementary amount of EG (corresponding to a molar ratio TEOS:EG=1:1), to the one necessary for the complex formation. Under these conditions, in the system will be enough EG for a quantitative formation of complexes.

All the M_i gels were examined by thermal analysis until 500°C, in air, registering the same thermal processes as for the E_i gels.

The results presented in Table 2, show that in the range 200–300°C in which the exothermic decomposition of the complex takes place, the mass losses are not proportional to the complexes concentration in the matrix. This fact is explained by the superposition in this temperature range of two processes: the decomposition of the complex and the decomposition of the organic chains from the matrix. Over 350°C, the mass of the samples maintains constant and the residue contains the metal oxides mixture in the pores of the silica matrix.

The thermal analysis shows that during the thermal treatment of the gels (TEOS–EG–MN), the redox reaction between EG and MN takes place forming in the pores of the silica matrix Fe(III), Ni(II), Zn(II) complex with glyoxylate ligand. At higher temperature, the oxidative decomposition of the complex takes place forming the oxides mixture embedded in the silica matrix. It also results that during the synthesis, EG chemically interacts with the functional groups of the silica matrix, leading to a hybrid matrix and influencing the ferrite nanoparticles formation.

Table 2 Thermal analysis results for the gels M_i thermally treated at 130°C

	M_1	M_2	M_3	M_4	M_5	M_6
Δm/%, 20–200°C	19	23	19	16	19	17
Δm/%, 200–300°C	21	15	22	23	27	28
Δm/%, 300–500°C	5	5	3	5	3	3
m_{res}/%, 500°C	55	57	56	56	51	52

FTIR analysis

By FTIR analysis we have followed the formation of the precursor complex combination of the Ni,Zn ferrite, in the silica matrix.

Figure 5 presents the FTIR spectra of the gels E_1, E_2, E_3, E_4, E_5, E_6 dried at 40°C. The corresponding spectra present all the bands characteristic to the matrix (3460, 1640, 1075 cm^{-1} with shoulder at 1200, 960, 800, 580 and 475 cm^{-1}) [17] as well as bands characteristic to the nitrate ion (at 1380 cm^{-1} intense) and to the ethylene glycol (at 2800–3000 and 880 cm^{-1}) present in the pores of the matrix as reagents for the formation of the complex combination [15].

Figure 6 shows the FTIR spectra of the gels E_i thermally treated at 130°C, which contains the glyoxylate type complex, formed as a result of the redox reaction between the nitrate ion and ethylene glycol. This is certified by the disappearance of the band at 1380 cm^{-1} characteristic to the NO_3^- ion, as a result of its consumption in the redox reaction. Also, in the range 1320–1420 cm^{-1} three characteristic bands of the complex combination of carboxylate type appear [13, 18]: $\nu_{s(CO)}$ at 1311 cm^{-1}, δ_{OH} at 1360 cm^{-1} and $\nu_{s(COO^-)}$ at 1400 cm^{-1}, excepting the spectra of the samples E_1 and E_2 (with low concentration of the complex).

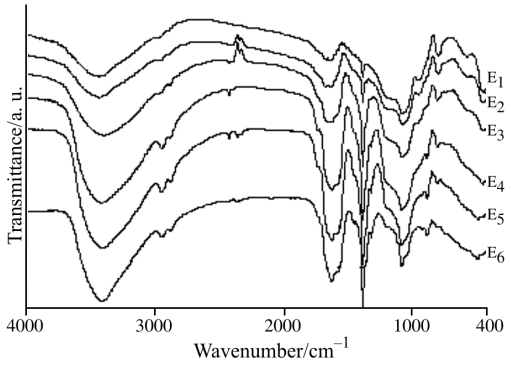

Fig. 5 FTIR spectra of the gels E_i (TEOS–MN–EG), of different compositions dried at 40°C

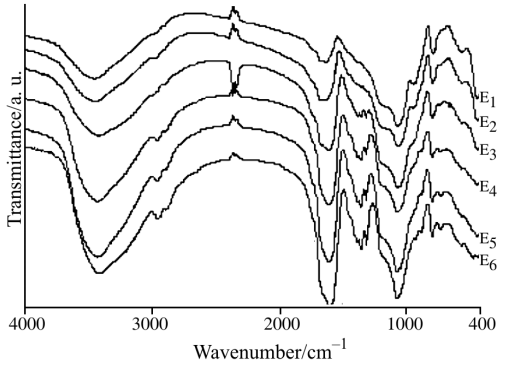

Fig. 6 FTIR spectra of the gels E_i (TEOS–MN–EG), of different compositions thermally treated at 130°C

The band at 1620 cm^{-1} characteristic to the $\nu_{as(COO^-)}$ vibration, overlaps with the one characteristic to water. The band characteristic to the ν_{C-OH} vibration of the carboxylic group, located at ~1060 cm^{-1} overlaps with the band $\nu_{Si-O-Si}$ characteristic to the matrix, leading to a more intense one.

XRD analysis

In order to obtain $(Ni_{0.65}Zn_{0.35}Fe_2O_4)_x/(SiO_2)_{100-x}$ nanocomposites (where x=10, 20, 30, 40, 50, 60 mass%), the gels M_i obtained at 130°C (containing the glyoxylate precursor) were thermally treated at different temperatures (600, 800, 1000°C) for 3 h.

XRD spectra of the samples thermally treated at 1000°C are shown in Fig. 7.

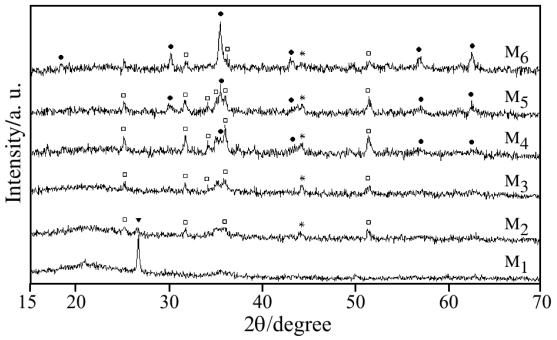

Fig. 7 XRD spectra of the powders obtained by calcinations at 1000°C, 3 h, of the M_i gels; ● – nickel–zinc–iron oxide, ▼ – quartz SiO_2, □ – fayalite syn $Fe_2(SiO_4)$, ∗ – nickel oxide hydroxid, Ni_2O_3H

The formation of Ni,Zn ferrite nanoparticles in silica matrix was investigated by XRD phase analysis. Diffraction peaks related to Ni,Zn ferrite with spinel structure appear in the XRD spectra of M_4, M_5 and M_6 samples (with 40, 50 and 60% ferrite in silica). Although the XRD spectra of M_1, M_2 and M_3 do not show any characteristic patterns of Ni,Zn ferrite, these samples exhibit characteristic magnetic properties. In this case it is obvious that the Ni,Zn ferrite consists on fine particles, which act as an amorphous phase.

Diffraction peaks related to other crystalline phases also appear in the XRD spectra of the samples M_i. Thus, on the M_1 spectra could be observed the characteristic patterns of quartz revealing the crystallization of silica matrix.

The XRD spectra of M_2–M_6 samples exhibit two additional phases Fe_2SiO_4 [19, 20] and Ni_2O_3H [21]. The presence of these phases in M_i samples could be explained by the characteristic feature of our synthesis method.

When the glyoxylate complex combination is embedded in silica matrix, FeO (formed by Fe(III) reduction during the thermal decomposition of the complex) interacts with SiO_2 at a certain temperature forming Fe_2SiO_4. This compound was identified by XRD analysis even for samples calcined at 600°C.

Unreacted nickel oxide (as a result of FeO consumption in the Fe_2SiO_4 formation) was observed as Ni_2O_3H phase in XRD spectra.

In order to avoid this drawback, all M_1–M_6 samples were calcined at 400°C, for 3 h. Thus, Fe(II) does not interact with SiO_2, but is reoxidized to Fe(III) forming amorphous Fe_2O_3 oxide, very reactive. Fe_2O_3 interacts with NiO and ZnO with formation of ferrite Ni,Zn crystallites. By subsequent calcination at higher temperature of the samples (calcined before at 400°C), Ni,Zn ferrite well crystallized was obtained in silica matrix, without any other secondary phases.

Figure 8 shows the XRD spectra of M_4 and M_6 samples calcined at 1000°C, for 3 h, (after a former thermal treatment at 400°C). In these spectra only Ni,Zn ferrite was evidenced as a crystallized phase, confirming the supposed mechanism for ferrites formation.

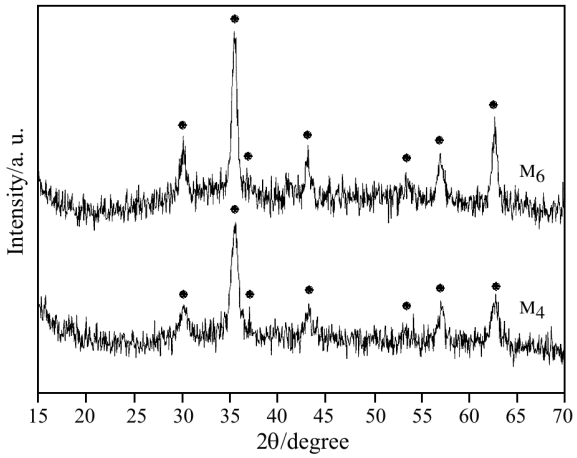

Fig. 8 XRD spectra of samples M_4 and M_6, thermally treated at 400°C, then calcined at 1000°C

The low intensity and the large full-width at half-length of diffraction maxima show, that the mean diameter of crystallites is in the range of nanometers. By calculation of mean diameter of nanoparticles with Scherrer formula [22], results that their dimension is in the 5–15 nm range.

With lowering of ferrite concentration inside the SiO_2 matrix, the mean diameter of nanoparticle will decrease as well.

Magnetic measurements

Magnetic properties of nanocomposites M_i with different compositions obtained at 1000°C were investigated in an external magnetic field. The presence of ferromagnetic phase was confirmed by magnetization

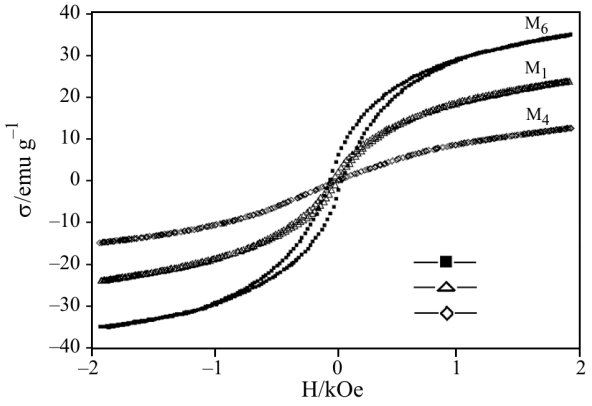

Fig. 9 Magnetization curves of the samples M_1, M_4, M_6 calcined at 1000°C, 3 h

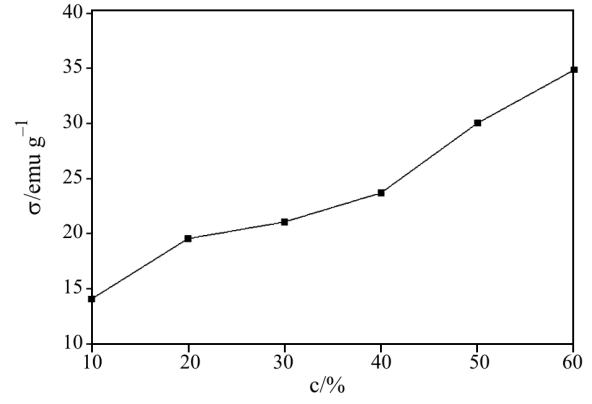

Fig. 10 Specific saturation magnetization (σ) variation with the Ni,Zn ferrite concentration (*c*/%) in the silica matrix

curves for all M_I samples. The magnetization curves for M_1, M_4 and M_6 samples are shown in Fig. 9.

The values of saturation specific magnetization (Fig. 10) lower than for bulk ferrite (78 emu g^{-1}) [23] correspond to ferromagnetic phase, as nanoparticules system. Magnetization is influenced by ferrite/matrix ratio, having lower values when the concentration of ferrite is low.

The nanocomposites behavior in an external magnetic field is influenced by ferrite/silica ratio (Figs 9 and 11).

The behaviour of synthesized nanocomposites in external magnetic field is a function of the ferrite percent in the silica matrix (Figs 9 and 11), and varies from superparamagnetic (SPM) (H_c=0) for M_1 (10% ferrite), to ferrimagnetic behaviour ($H_c \neq 0$) for the other compositions. The values and variations of the coercive field (Fig. 11) confirm the presence of ferrimagnetic nanoparticles in the silica matrix. The presence of the fayalite paramagnetic phase [19, 20] does not influence (affect) the magnetic behaviour at room temperature of the Ni,Zn ferrite nanoparticles, since there is a difference of two orders in magnitude between their magnetic properties.

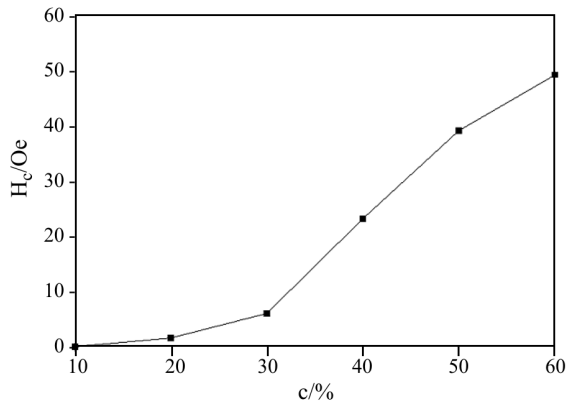

Fig. 11 The variation of coercive field (H_c) with the Ni,Zn ferrite concentration (*c*/%) in the silica matrix

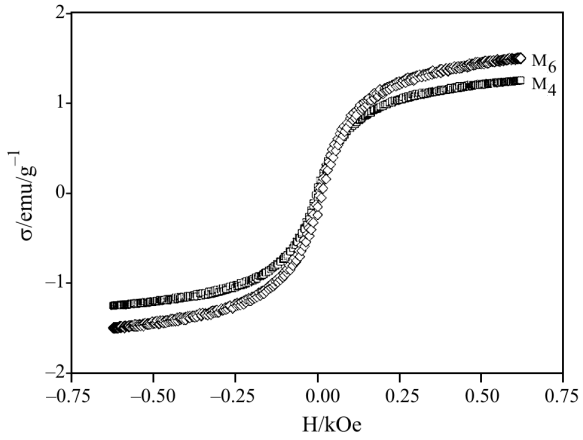

Fig. 12 Magnetization curves of the samples M_4 and M_6 treated at 400°C, then calcined at 1000°C

For the samples M_1–M_6 treated first at 400°C, and then calcined at 1000°C, when the XRD spectra show the Ni,Zn ferrite as the only phase (Fig. 8), the magnetization curves (Fig. 12) do not show any hysteretic loop, characteristic for a super paramagnetic behaviour.

This magnetic behaviour (H_v=0), together with the low values for the saturation magnetization, confirms the presence of ferrite as fine nanoparticles (d<10 nm) inside the silica matrix, according to the XRD spectra.

These results of the magnetic measurements show that the magnetic properties of the synthesized $(Ni_{0.65}Zn_{0.35}Fe_2O_4)_x/(SiO_2)_{100-x}$ nanocomposites can be controlled and perfected by thermal treatment and variation of the ferrite concentration in the silica matrix.

Conclusions

This study regards the obtaining of $(Ni_{0.65}Zn_{0.35}Fe_2O_4)_x/(SiO_2)_{100-x}$ nanocomposites, by thermal decomposition of the glyoxylate type com-

plex resulted in the pores of the silica matrix from the redox reaction between EG and metallic nitrates. The interaction of ethylene glycol with the hydrolysis products of TEOS with formation of a hybrid matrix was evidenced by thermal analysis. This interaction influences the obtaining of the glyoxylate type precursor as well as the formation of the ferrite nanoparticles in the pores of the silica matrix.

The thermal decomposition of the glyoxylate type complex embedded in the silica matrix, takes place with reduction of Fe(III) at Fe(II) forming FeO. During the thermal treatment, FeO reacts with SiO_2, from the matrix, leading to the formation of a secondary phase (Fe_2SiO_4). In order to avoid Fe_2SiO_4 formation, the decomposition of the gloxylate type precursor and the thermal treatment have to be carefully controlled. In this case, the unique phase obtained in the matrix is Ni,Zn ferrite.

The control on the synthesis parameters allows the obtaining of Ni,Zn ferrite, in the matrix, as very fine nanoparticles (d<10 nm).

The study shows that the magnetic properties of the synthesized nanoparticles depend on the Ni,Zn ferrites concentration in the SiO_2 matrix, but they can be controlled and perfected by the synthesis parameters.

Acknowledgements

This paper was supported from the CNCSIS A 648/2006 and CNCSIS A 728/2006 grants, by the programm MEdC, Romania.

References

1 D. Sen, P. Deb, S. Mazumader and A. Basumallik, Mater. Res. Bull., 35 (2000) 1243.
2 J. H. Paterson, R. Devine and A. D. R. Phelps, J. Magn. Magn. Mater., 196 (1999) 394.
3 R. Mathur, M. Parihar, S. R. Vadera and N. Kumar, J. Magn. Soc., 22 (1998) 273.
4 A. Chatterjee, D. Das, D. Chakravorty and K. Choudhury, Appl. Phys. Lett., 57 (1990) 1360.
5 K. H. Wu, Y. C. Chang and G. P. Wang, J. Magn. Magn. Mater., 269 (2004) 150.
6 K. H. Wu, C. H. Yu, Y. C. Chang and D. N. Horng, J. Solid State Chem., 177 (2004) 4119.
7 K. H. Wu, Y. C. Chang, H. B. Chen, C. C. Yang and D. N. Horng, J. Magn. Magn. Mater., 278 (2004) 156.
8 J. B. da Silva and N. D. S. Mohallem, J. Magn. Magn. Mater., 226–230 (2001) 1393.
9 R. D. Shull, J. J. Ritter and L. J. Swarlzendruber, J. Appl. Phys., 69 (1991) 5144.
10 X. He, Q. Zhang and Z. Ling, Mater. Lett., 57 (2003) 3031.
11 K. H. Wu, T. H. Ting, M. C. Li and W. D. Ho, J. Magn. Magn. Mater., 298 (2006) 25.
12 C. Caizer, J. Phys.: Condens. Mater., 15 (2003) 765.
13 M. Ştefanescu, C. Caizer, C. Muntean, M. Stoia and M. Bîrzescu, Chem. Bull. 'Politehnica' Univ. (Timişoara), 45 (2000) 30.
14 C. Caizer and M. Stefanescu, J. Phys. D: Appl. Phys., 35 (2002) 3035.
15 M. Stefanescu, C. Caizer, M. Stoia and O. Stefanescu, Acta Mater., 54 (2006) 1248.
16 M. Stefanescu, M. Stoia and O. Stefanescu, J. Sol-Gel Sci. Technol., (2007), in press.
17 R. F. S. Lenza and W. L. Vasconcelos, J. Non-Cryst. Solids, 330 (2003) 216.
18 R. Prasad, Sulaxna and A. Kumar, J. Therm. Anal. Cal., 81 (2005) 441.
19 H. Fuess, O. Ballet and W. Lottermoser, Minerals, S. Ghose, I. M. D. Coey and E. Salje, Eds, Berlin 1988.
20 M. Cococcioni, A. D. Corso and S. Gironcoli, Phys. Rev., 67 (2003) 94106.
21 A. M. Malsbury and C. Greaves, J. Solid State Chem., 71 (1987) 418.
22 H. P. Klug and L. E. Alexander, X-ray Diffraction Procedure, Wiley, New York 1974.
23 J. Smit and H. P. J. Wijin, Les ferrites, Bibl. Tech. Philips, Paris 1961.

DOI: 10.1007/s10973-006-8004-5